applied sciences

MDPI

Article

Spectral and Spatial Analysis of Plantar Force Distributions Across Foot-Strike Patterns During Treadmill Running

Paul William Macdermid * and Stephanie Julie Walker

School of Sport, Exercise and Nutrition, College of Health, Massey University, Palmerston North 4472, New Zealand; stephanie.walker.9@uni.massey.ac.nz
* Correspondence: p.w.macdermid@massey.ac.nz

Abstract

Treadmill running gait differs to overland running and is commonly used to evaluate interventions. One challenge is accurately defining strike pattern and related impact kinetics. This study aimed to characterise foot-strike patterns during treadmill running using the spatial distribution of in-shoe plantar forces and to identify differences in impact kinetics through spectral analysis. Low- and high-frequency power components were analysed in heel, midfoot and forefoot strike patterns. No distinct impact peaks were identified in the force traces; however, significant spatial differences were found. Forefoot strikes exhibited lower peak impact force, average loading rate, and high-frequency power spectral density (PSD) components compared to heel and midfoot strikes, with heel also lower than midfoot. Strike pattern classification was derived from spatial force distribution, where >70% posterior and >50% anterior denote heel and forefoot strikes, while midfoot strikes demonstrate a more balanced distribution with >25% in the central zone. These findings support the integration of spatial, force-based classification with frequency-domain analysis to enhance the evaluation of impact attenuation in treadmill-based running interventions.

Keywords: running; gait; foot-strike; ground reaction forces

Academic Editor: Mark King

Received: 10 July 2025
Revised: 1 August 2025
Accepted: 5 August 2025
Published: 6 August 2025

Citation: Macdermid, P.W.; Walker, S.J. Spectral and Spatial Analysis of Plantar Force Distributions Across Foot-Strike Patterns During Treadmill Running. *Appl. Sci.* **2025**, *15*, 8709. https://doi.org/10.3390/app15158709

1. Introduction

Runners have distinctive footstrike patterns classified as heel, midfoot, or forefoot [1]. Typically, elite runners are forefoot strikers [2], yet over 90% of recreational runners are expected to be heel strikers [2]. Visually, it requires high-speed video [3] to capture the specific region of the foot that makes initial contact with the ground [4]. However, this method does not reveal the distribution of plantar forces. Alternatively, it can be inferred from foot centre of pressure, vertical ground reaction force [5] and more recently tri-axial accelerometers [6].

In vertical ground reaction force traces, the presence of two force peaks indicates a heel or mid-foot strike (Figure 1A,B). A large first peak signifies a heel strike, a smaller more rounded peak is a midfoot strike, and no peak signifies a forefoot strike [7,8] (Figure 1C).

These landmarks are important as they reflect the early impact absorption phase of stance, where passive structures absorb ground contact forces. This phase precedes active muscle engagement [9] and captures the unattenuated collision between the foot and ground [10]. While such patterns are typically derived from overground running, treadmill running involves no net displacement of the runner. As a result, the average velocity of the centre of mass relative to the laboratory frame is zero [11], and joint kinematics differ during the stance phase [12]. However, since the advent of instrumented treadmills [13],

ground reaction force profiles at matched speeds are generally similar [14], although some variability may occur between treadmill brands or when compared to in-shoe pressure insoles [15]. Furthermore, peak plantar pressures are generally lower during treadmill running, though pressure distribution remains similar [16]. These modality differences may influence strike-pattern classification [17] and impact-related metrics derived from them.

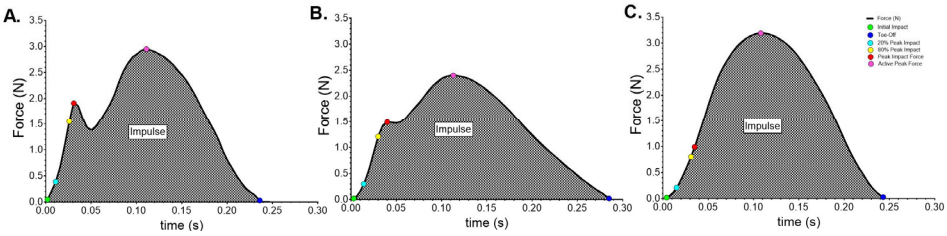

Figure 1. Examples of running strike patterns running at 14 km·h^{-1} overground using the same running shoe design. (**A**): Heel, (**B**): midfoot, and (**C**): forefoot strikes. Unpublished data collected within our research group.

The magnitude and loading rate of collision forces have been extensively studied for association with high injury rates and attenuation efficacy of midsole cushioning in runners [10,18–24]. However, in both cases the links are tenuous, where higher impact forces and loading rates are seen in heel strikes, compared to midfoot or forefoot strikers [25]. Likewise, research into the effectiveness of shoe cushioning properties is somewhat inconclusive. Questions have been raised [26] regarding the efficacy of traditional kinetic metrics used as indicators of foot-strike mechanics [5] and impact severity. The authors highlighted how total force measurements may obscure footwear-related effects [26]. Additionally, the reliance on total peak values may overlook the spectral composition of the force signal. Low-frequency components (<10 Hz), which are more related to the active processes rather than impact [27], can hide [26] the high-frequency content (>10 Hz) more associated with impact and caused by the limb's rapid movement [28].

Therefore, the aim of this study is to characterise foot-strike patterns during treadmill running via spatial distribution of in-shoe plantar forces, and to identify differences in impact kinetics through spectral analysis of low- and high-frequency components.

2. Materials and Methods

2.1. Participants

Eleven recreational to nationally competitive endurance runners, free of injury, participated in the study after providing written consent in accordance with the University Human Ethics Committee approval. This sample size was based on priori statistics (G*power V 3.1.9.7, Heinrich-Heine University, Dusseldorf, Germany) for analysis of variance (ANOVA) repeated measures within factors, using an alpha value of 0.05, power of 0.95, and effect sizes based on previously reported differences in foot strike patterns and kinetic variables: peak impact force, 2.43 [23]; heel pressure, 1.08 [26]; loading rate, 1.62–2.44 [23,29,30]; active peak force, 0.56–1.41 [5,23,29].

Participant characteristics (mean ± SD): age 29.6 ± 9.8 years, height 174.0 ± 8.7 cm, body mass 65.4 ± 8.9 kg and Body Mass Index 21.5 ± 1.3, and weekly training volume 77.3 ± 23.6 km·wk^{-1}.

Prior to the study, participants exhibited baseline individual peak impact force distributions during treadmill running at 12 km·h^{-1} (Figure 2). The mean ± SD step count was 138 ± 10, with heel, midfoot, and forefoot components of 47.7 ± 29.4%, 29.1 ± 10.4, forefoot component (%) 23.2 ± 15.6.

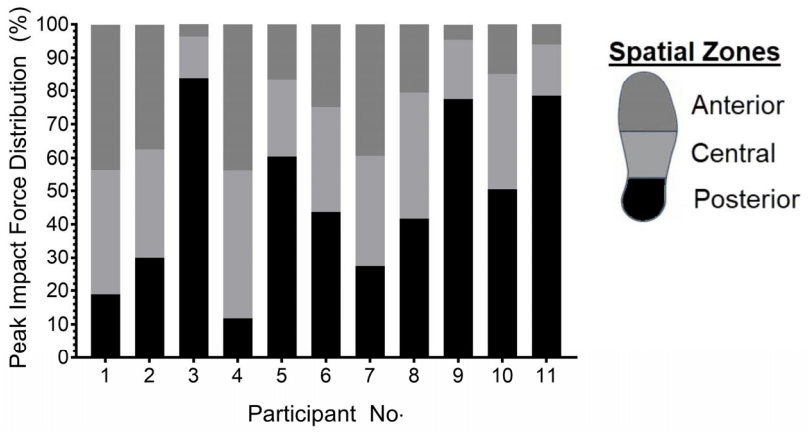

Figure 2. Baseline spatial distribution of peak impact force during 12 km·h^{-1} treadmill running for each participant.

2.2. Procedures and Measurements

The experimental protocol consisted of three trials (heel, midfoot, and forefoot strike patterns) while treadmill running at 10 km·h^{-1}. Each trial was performed in one session on the same day, with strike pattern conditions presented in a counter balanced order. All participants wore the same familiar (>20 km of running) brand-model of footwear throughout testing.

Upon arrival at the laboratory, participants were weighed, measured and presented with the required shoe size. The prototype cushioned shoe (Figure 3A) has a 38 mm heel stack height, measured at 12% of the shoe's total length from the heel, and a 32 mm forefoot stack height, measured at 75% of the total shoe length from the same reference point. The midsole consists of a single layer of Aliphatic Thermoplastic Polyether Polyurethane (ATPU) super critical bead foam cushioning. This is a lightweight cushioning foam produced through injecting supercritical fluid to create a uniform microcellular structure. The foam had a factory pre-processing density of 0.08 ± 0.01 g·cm^{-2}. Shoe cushioning property assessment using a modified industry standard test (ISO 20344:2021 (5.17)) [31]—Instron 4467 (Instron, Norwood, MA, USA)—compressed the midsole vertically at a rate of 10 mm per minute with a maximum applied force of 2.2 kN. Results of this test are provided in Figure 3B.

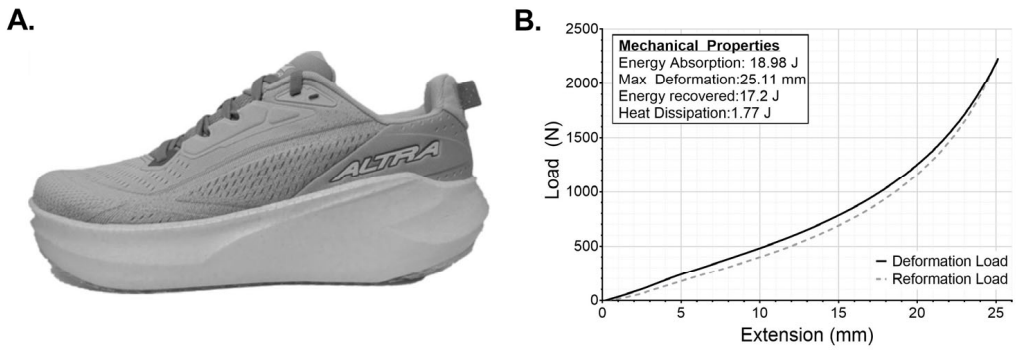

Figure 3. (**A**). The test footwear and (**B**) the load–extension profile illustrating the midsole energy absorption and hysteresis behaviour.

Following a self-selected warm-up period on the treadmill (Life Fitness, Hamilton, New Zealand) at 10 km·h^{-1}, participants were asked to use one of three strike pattern techniques (Heel, Midfoot, or Forefoot). Prior to and during each trial, where necessary, instructions were given to land (make initial contact) on:

- Heel strike, letting the heel touch down first before the rest of the foot.
- Midfoot strike, land with your whole foot touching down nearly at once, i.e., flatfooted.
- Fore-foot strike, land on the balls of your feet.

Once they were comfortable and had been running for at least 1 min with the specified technique, and this was verified through a real-time force trace, 10 s of data were logged for each condition [31,32].

Time-force data from Loadsol® pressure-sensitive in-soles (novel gmbh, Munich, DE, Germany), segmented into posterior, central, and anterior zones based on the manufacturer's predefined sensor configuration (Figure 2), was logged at 200 Hz. The insoles were size matched to each participant's foot, ensuring boundaries were standardised according to insole design. The data was then uploaded to MATLAB (R2022b, (MathWorks, Inc., Natick, MA, USA), re-sampled to 1000 Hz, and processed using a 10–20 N force threshold to detect initial foot contact and toe-off in the total force trace. Based on these identified points, the following variables were identified or calculated [31], including spatial zone data where applicable:

1. Stride duration was the time from one initial impact to the next initial impact for the same foot.
2. Ground contact time (s) was the time the foot remained in contact with the treadmill surface, i.e., toe-off–initial contact times.
3. Swing time (s) was the time the foot has no contact with the treadmill surface.
4. Active peak vertical force ($N \cdot BW^{-1}$) was the second peak for heel strike runners, or the highest force reading of each step for midfoot and forefoot strikers.
5. Peak vertical impact force ($N \cdot BW^{-1}$) identified as the first peak in the total force trace between initial contact and the active peak. If the first peak was not present in running (mid-forefoot strike), it was defined as the force at 13% of the ground contact time.
6. Average loading rate ($N \cdot BW^{-1} \cdot s^{-1}$) is the difference between forces at 20% and 80% of the peak impact force divided by the corresponding time interval (s).
7. Impulse ($N \cdot s \cdot BW^{-1}$), the area under the force–time curve.
8. Power Spectral Density (PSD) analysis: During the stance phase, while the right foot was in contact with the ground, force data (total and spatial zones) were analysed in the frequency domain. PSD was computed using Welch's [33] method (MATLAB, default windowing), and applied to the first 20% of each step's stance phase to isolate impact-related portion of ground contact. A frequency resolution of 2 Hz was used from 0 to 100 Hz. PSD values were retained in their raw form ($N^2 \cdot Hz^{-1}$), preserving magnitude to reflect actual spectral energy differences across the zones in relation to strike pattern. Spectral power was partitioned into low-frequency (<10 Hz) and high-frequency (10–100 Hz) bands to quantify relative contributions and frequency-dependent loading characteristics.

2.3. Statistical Analysis

All dependent variable data were calculated per step and expressed as mean ± SD for each independent variable. Differences in spatiotemporal and kinetic parameters determined from total force were compared between strike patterns using a one-way ANOVA, with Tukey post hoc multiple comparisons if significance was found. Differences between strike pattern and spatial zones and or low-frequency and high-frequency bands were analysed using a two-way repeated-measures ANOVA, with 2 within-subject variables (strike-pattern*Spatial-zone) or (strike-pattern*Frequency-band). Where significance was found, Sidak's post hoc multiple comparisons testing was performed. All statistics were performed using GraphPad Prism V 8.4 (GraphPad Software, San Diego, CA, USA) with significance set at $p < 0.05$.

3. Results

The data analysis period resulted in the analysis of 13 ± 1, 14 ± 1 right steps for the heel/midfoot, and forefoot strike patterns, respectively. No distinct initial impact peaks were observed in any foot-strike method for any participant despite there being clear spatial differences, as shown in Figure 4.

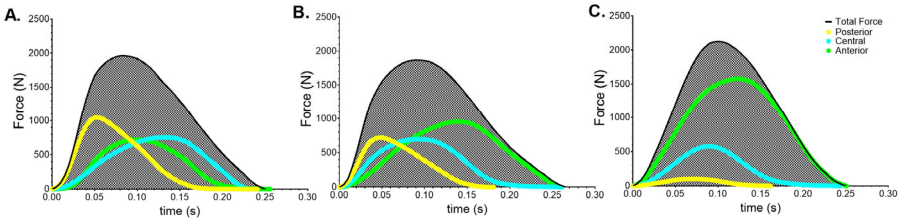

Figure 4. Plantar force traces from participant 10 for total, posterior, central, and anterior zones whilst using (**A**) heel, (**B**) midfoot, and (**C**) forefoot strike pattern.

Mean ± SD data for total force-derived variables stride duration, ground contact time, swing time, peak impact force, average loading rate, active peak force, and impulse are presented in Table 1. One-way ANOVA found no significant differences for stride duration ($F_{(1.76,17.65)} = 1.6$, $p = 0.230$), ground contact time ($F_{(1.85,18.47)} = 1.05$, $p = 0.365$), or swing time ($F_{(1.85,18.47)} = 0.98$, $p = 0.389$). There were overall significant differences for peak impact force ($F_{(1.63,16.25)} = 13.58$, $p = 0.0006$, Table 1) with forefoot impact being less than heel ($p = 0.024$) and midfoot ($p = 0.002$) strike patterns; average loading rate ($F_{(1.75,17.54)} = 14.61$, $p = 0.0003$), with forefoot being less than heel ($p = 0.009$) and midfoot ($p = 0.001$) strike patterns; active peak force ($F_{(1.36,13.55)} = 20.32$, $p = 0.0002$, Table 1) with the heel being less than both midfoot ($p = 0.023$) or forefoot ($p = 0.001$), and the midfoot less than the forefoot ($p = 0.006$); impulse ($F_{(1.11,11.05)} = 23.9$, $p = 0.0004$, Table 1) with the heel being less than the midfoot ($p < 0.0001$), and the forefoot ($p = 0.0008$), while the midfoot was also less than the forefoot ($p = 0.012$) strike patterns.

Table 1. Mean ± SD spatiotemporal and kinetic variables generated from total force for each strike pattern.

	Strike Pattern		
	Heel	**Mid-Foot**	**Fore-Foot**
Stride duration (s)	0.762 ± 0.035	0.753 ± 0.043	0.760 ± 0.039
Ground contact time (s)	0.257 ± 0.018	0.253 ± 0.012	0.253 ± 0.015
Swing time (s)	0.505 ± 0.049	0.500 ± 0.052	0.508 ± 0.050
Peak Impact Force ($N \cdot BW^{-1}$)	1.64 ± 0.35	1.74 ± 0.31	1.37 ± 0.34
Average Loading Rate ($N \cdot s^{-1} \cdot BW^{-1}$)	53.7 ± 16.1	55.3 ± 13.2	39.11 ± 12.6
Active Peak Force ($N \cdot BW^{-1}$)	2.93 ± 0.35	3.04 ± 0.30	3.31 ± 0.26
Impulse ($N \cdot s \cdot BW^{-1}$)	0.45 ± 0.03	0.47 ± 0.03	0.49 ± 0.03

Two-way ANOVA for peak impact identified a strike-pattern*Spatial-zone interaction ($F_{(4,40)} = 91.12$, $p < 0.0001$, Figure 5) with a main effect for strike pattern ($F_{(2,20)} = 14.14$, $p = 0.0001$) and spatial zone ($F_{(2,20)} = 13.37$, $p = 0.0002$). Within each strike pattern multiple post hoc comparisons (Figure 5A, Table 2) presented increased contribution of the posterior zone compared to either the central or anterior zone ($p < 0.0001$) during heel striking; increased contribution of the posterior compared to the central or anterior zones ($p < 0.01$) during midfoot strikes; while the anterior zone was greater ($p < 0.0001$) than

either the central or posterior zones during forefoot strikes. Between strike pattern comparisons for the major zone of force contribution showed that the posterior zone in heel strikes was greater than the posterior in the midfoot or anterior zone in the forefoot strikes ($p < 0.0001$). From a contribution perspective, the Mean ± SD (%) values for posterior, central and anterior zones were heel strikes—81 ± 13, 16 ± 11, 3 ± 3; midfoot strikes—49 ± 19, 29 ± 11, 21 ± 10; and forefoot strikes—9 ± 15, 28 ± 9, 63 ± 17, respectively (Figure 5C). As such, the overall spatial zone contribution was significantly different for each foot strike ($F_{(2,20)} = 10.27$, $p = 0.0009$, Figure 5C) where post hoc analysis identified significance ($p < 0.05$) in every pairing except between the central and anterior zones in the heel and midfoot strikes.

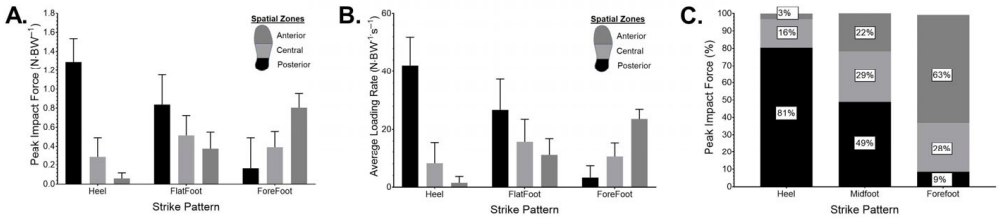

Figure 5. Mean ± SD data for each strike pattern for (**A**) spatial component of vertical peak impact force ($N \cdot BW^{-1}$), (**B**) spatial component of average loading rate ($N \cdot s^{-1} \cdot BW^{-1}$), (**C**) mean percentage contribution of spatial components to total vertical peak impact force.

Table 2. Mean ± SD for kinetic variables for the spatial zones across strike patterns.

	Strike Pattern								
	Heel			**Mid-Foot**			**Fore-Foot**		
Spatial Zone	Posterior	Central	Anterior	Posterior	Central	Anterior	Posterior	Central	Anterior
Peak Impact Force ($N \cdot BW^{-1}$)	1.29 ± 0.25	0.28 ± 0.21	0.17 ± 0.33	0.84 ± 0.31	0.52 ± 0.21	0.17 ± 0.33	0.17 ± 0.33	0.39 ± 0.17	0.81 ± 0.15
Average Loading Rate ($N \cdot s^{-1} \cdot BW^{-1}$)	42.16 ± 9.70	8.17 ± 7.32	1.15 ± 2.15	26.68 ± 10.63	15.76 ± 7.71	11.01 ± 5.81	3.28 ± 4.05	10.46 ± 4.92	23.58 ± 3.31
Active Peak Force ($N \cdot BW^{-1}$)	1.06 ± 0.03	0.98 ± 0.23	0.89 ± 0.11	0.64 ± 0.28	0.97 ± 0.24	1.43 ± 0.26	0.18 ± 0.22	0.82 ± 0.34	2.12 ± 0.53
Impulse ($N \cdot s \cdot BW^{-1}$)	0.16 ± 0.03	0.12 ± 0.03	0.17 ± 0.02	0.09 ± 0.04	0.12 ± 0.03	0.25 ± 0.04	0.02 ± 0.03	0.10 ± 0.04	0.37 ± 0.05

The two-way ANOVA for average loading rate identified a strike-pattern*Spatial-zone interaction ($F_{(4,40)} = 74.7$, $p < 0.0001$, Figure 5B, Table 2) with a main effect for strike pattern ($F_{(2,20)} = 11.24$, $p = 0.0007$) and spatial zone ($F_{(2,20)} = 22.9$, $p < 0.0001$). Within each strike pattern multiple post hoc comparisons (Figure 5B, Table 2) presented increased contribution of the posterior > central or anterior zone ($p < 0.0001$) during heel striking; the posterior > central ($p = 0.002$) or anterior zones ($p < 0.0001$) during midfoot strikes; and the anterior > central ($p < 0.0001$) > posterior ($p < 0.0001$) zone in the forefoot strikes.

Two-way ANOVA (strike-pattern*spatial-zone) for active peak force resulted in an interaction ($F_{(4,40)} = 59.17$, $p < 0.0001$) with a significant effect for spatial zone ($F_{(2,20)} = 35.84$, $p < 0.0001$) but not strike pattern ($F_{(2,20)} = 0.94$, $p = 0.406$). Multiple post hoc comparisons for spatial zone across strike patterns highlighted significance ($p < 0.001$) for the posterior and anterior zones but not the central zone ($p > 0.8$), as shown in Table 2. Impulse had an interaction ($F_{(4,40)} = 104.4$, $p < 0.0001$) with main effect differences for both strike pattern ($F_{(2,20)} = 20.88$, $p < 0.0001$) and spatial zone ($F_{(2,20)} = 76.8$, $p < 0.0001$) with $p < 0.0001$ post hoc differences for both posterior and anterior zones but not the central zone ($p > 0.8$), as shown in Table 2.

PSD analysis (Figure 6) showed a frequency*strike-pattern interaction ($F_{(2,20)} = 11.74$, $p = 0.0005$) with a main effect for frequency ($F_{(1,10)} = 136.4$, $p < 0.0001$) and strike pattern ($F_{(2,20)} = 12.37$, $p = 0.0004$). Post hoc comparisons between strike patterns were not signifi-

cantly different in the low-frequency band but there were different in the high-frequency band for all pairings (Figure 6A). Specifically, total high frequency was lower in the heel strike compared to midfoot strike (255,351 ± 79,702, 302,406 ± 100,656 $N^2 \cdot Hz^{-1}$, $p = 0.011$), heel strike was greater than the forefoot strike (255,351 ± 79,702, 185,948 ± 51,238 $N^2 \cdot Hz^{-1}$, $p = 0.0004$) and the midfoot was greater than the forefoot strike (302,406 ± 100,656, 185,948 ± 51,238 $N^2 \cdot Hz^{-1}$, $p < 0.0001$). Further analysis of the high-frequency component with regards to strike-pattern*spatial-zone (Figure 6B) showed an interaction ($F_{(2,20)} = 65.6$, $p < 0.0001$), and main effects for both strike pattern ($F_{(2,20)} = 16.91$, $p < 0.0001$) and spatial zone ($F_{(1,10)} = 28.47$, $p < 0.0001$). Key post hoc comparisons of interest highlighted greater PSD high frequency in the heel strike posterior zone vs. midfoot strike central zone (166,845 ± 48,401, 32,613 ± 18,687 $N^2 \cdot Hz^{-1}$, $p < 0.0001$), heel posterior vs. forefoot anterior (166,845 ± 48,401, 88,075 ± 30,093 $N^2 \cdot Hz^{-1}$, $p < 0.0001$), and heel posterior vs. midfoot central (166,845 ± 48,401, 77,517 ± 44,168 $N^2 \cdot Hz^{-1}$, $p < 0.0001$). There was no post hoc difference between midfoot central and forefoot central (32,613 ± 18,687, 18,082 ± 15,512 $N^2 \cdot Hz^{-1}$, $p < 0.0001$) or midfoot posterior and forefoot anterior (77,517 ± 44,168, 88,075 ± 30,093 $N^2 \cdot Hz^{-1}$, $p = 0.990$).

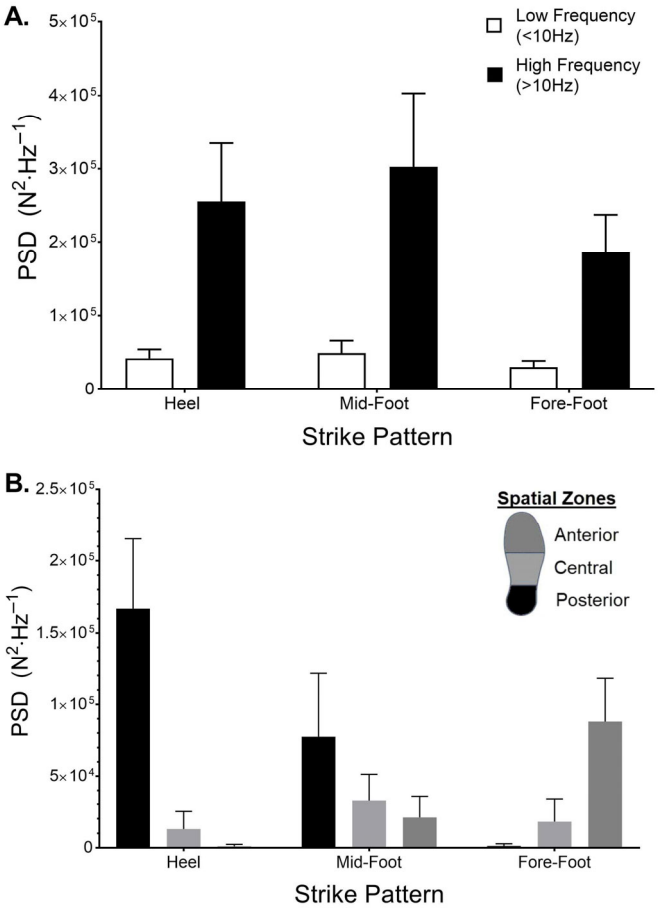

Figure 6. Mean ± SD data from power spectral density (PSD) of plantar forces for each strike pattern. (**A**). Comparison of the low-frequency (<10 Hz) and high-frequency (>10 Hz) PSD components, (**B**) high-frequency PSD distribution for the posterior, central, and anterior zones of the foot.

4. Discussion

This study aimed to evaluate spatial and spectral plantar forces across foot-strike patterns. While no significant stride duration, ground contact time or swing time variations occurred between foot strike patterns, significant spatial differences in peak impact and average loading rate were evident, despite the absence of distinct peaks in the midfoot or

heel strike total force traces. As such, strike classification based on spatial data is more accurate than total plantar force during treadmill running. Further, the total high-frequency component of the PSD was greatest in midfoot and lowest in the forefoot strikes, with the posterior zone of heel strikes exhibiting largest individual zone power. Lastly, total peak active force and total impulse were greater in forefoot strikes than in midfoot and heel strikes.

All participants were well trained, running ~70 km·wk^{-1} at the time of the study, and successfully adopted the assigned footstrike techniques, as evidenced by the plantar force profiles. This level of experience and technique adaptability reinforces reliability of the dataset, enabling us to develop classification guidelines based on spatial distribution of impact forces specific to treadmill running (Figure 5C). Runners exhibiting >70% of impact in the posterior zone were classified heel strikers; >50% in the anterior zone as forefoot strikers; and those with <70% posterior, <50% anterior, but >25% in the central zone were classified as midfoot strikers. Based on these classification thresholds, our retrospective analysis of the cohort included four natural heel strikers and seven natural midfoot strikers (Figure 2).

The adaptation of different strike patterns resulted in no within-subject differences to stride duration or its components, ground contact time or swing time. This agrees with comparisons between non-paired natural heel and forefoot strikers [34,35] and paired natural heel and unnatural forefoot strikers [30], and reflects a preferred movement path [36], whereby individuals modulate impact attenuation or force production from strike-specific spatial zones (Figure 5A,B, Table 2). However, this contrasts to observations where midfoot strikers presented shorter duration ground contact times and superior running economy than heel strikers [37]. In the current study, participants wore a prototype shoe that, in in vitro testing, i.e., mechanical testing without participants (Figure 3B), demonstrated approximately 11% greater cushioning than a maximally cushioned shoe, tested under the same conditions [31]. Given the association between footwear geometry and reduced ground contact time [38], as well as the influence of cushioning on leg stiffness and gait adaptations [39,40], such a design may have influenced strike pattern-related spatiotemporal variables. However, no differences were observed in the current dataset, aligning with comparisons between minimalistic and conventional cushioned shoes [8,41]. This supports previous work suggesting strike pattern, rather than shoe condition, has a greater effect on plantar pressures [42]. Further investigation exploring the interaction between shoe geometry, cushioning, and strike pattern is warranted.

The absorption phase of ground contact is characterised by impact kinetics, typically determined through force-trace peak identification [5] or a time component (<0.05 s) and the passive nature of damping [9]. While the first peak is always present in overground running, this criteria is somewhat equivocal during treadmill running [17], where both instrumented-treadmill brand, and kinetic measurement systems, have produced presence and absence of such peaks [15]. Data from the current study suggests that relying on total vertical force traces may lead to misclassification of strike patterns. Specifically, in-shoe total plantar force data revealed no distinct impact peaks for midfoot or heel strike peaks (Figure 4), despite clear distinctions in spatial zone differences in peak impact and average loading rate (Figure 5). These spatial differences aligned consistently with the designated strike pattern (Figure 5A,B). The posterior zone exhibited the highest-magnitude impact peak and average loading rate in the heel strike, the anterior zone dominated in the forefoot strike, and midfoot strike displayed a more even distribution where the posterior zone remained dominant (Figure 5). These within-strike pattern distinctions highlight the value of using spatial force data to accurately identify foot strike pattern and advanced spatial and spectral analysis to assess impact kinetics during running interventions.

Spectral analysis has been used to separate the true (high-frequency) impact component of the total force signal from that of the active processes [26,27] that occur during limb deceleration. Figure 6A supports the presence of a low-frequency active process component but suggests it may not significantly influence the overall kinetic signal. Alternatively, it could be that within the same participants, strike pattern did not alter the active processes. Nonetheless, strike pattern had a significant effect on peak impact, average loading rate (Table 1), and the high-frequency PSD. Interestingly, the midfoot strike had significantly greater values than either the heel or forefoot strike, despite most participants being natural midfoot strikers (Figure 2) based on the classification criteria (Figure 5C). This contrasts with previous research that has focussed on natural strike pattern preferences or overground running, which reports lower impact kinetics in midfoot and forefoot striker patterns [6,27,43]. It is possible that the instructions given to run flat-footed produced a gait distinct from participants' habitual midfoot style, potentially increasing vertical limb acceleration and thereby amplifying impact deceleration. This is supported where peak impact accelerations were greater in midfoot than rear or forefoot strike patterns [44]. However, stride duration, ground contact time and swing time showed no significant differences across conditions, suggesting that gross temporal mechanics remained stable. Although not a primary focus, the small, non-significant decrease in swing time (Table 1) warrants further exploration from a kinematic perspective. Additionally, spatial analysis of the high-frequency component revealed similarity with peak impact (Figure 5A) and average loading rate (Figure 5B), but with notable differences in zone contributions. Specifically, in the heel and forefoot strikes, non-dominant zones contributed less (Figure 6B). This suggests that the low-frequency components may inflate non-specific zone data during impact.

Although this study primarily focused on comparing strike pattern with respect to impact kinetics and force signal characteristics, active peak force associated with propulsion was also measured. The results showed significantly lower active peak force in heel strikes compared to midfoot and forefoot strikes, in both total and spatial zone measures (Tables 1 and 2). These findings contrast with previous work where there were no differences between total forces across strike patterns [43]. However, the data presented shows considerable posterior and central zone contributions to total force in both heel and midfoot strikes, indicating differences in plantar surface mechanics.

While no spatiotemporal differences were observed between foot-strike patterns using this specific shoe during treadmill running, and total force trace structure appeared similar when measured by in-shoe devices, distinct differences for impact kinetic variables between strike patterns were present, particularly when examined using frequency domain analysis. These distinct kinetic differences, combined with the ability to classify strike pattern based on spatial force metrics, could be used to discern intervention effects in treadmill running studies exploring different shoes and foot-strike characteristics, where previous findings have been equivocal.

Author Contributions: Conceptualization, P.W.M.; methodology, S.J.W. and P.W.M.; software, P.W.M.; formal analysis, P.W.M.; investigation, P.W.M. and S.J.W.; resources, S.J.W. and P.W.M.; data curation, P.W.M.; writing—original draft preparation, P.W.M.; writing—review and editing, S.J.W.; visualization, P.W.M.; project administration, P.W.M. and S.J.W. All authors have read and agreed to the published version of the manuscript.

Funding: This research received no external funding.

Institutional Review Board Statement: The study was conducted in accordance with the Declaration of Helsinki, and approved by the Ethics Committee of Massey University (OM1 24/44 approved 12 June 2025).

Informed Consent Statement: Informed consent was obtained from all subjects involved in the study.

Data Availability Statement: The raw data supporting the conclusions of this article will be made available by the authors on request.

Acknowledgments: We would like to acknowledge the support of Altra Running for the provision of the shoes used within this research, and Aden Murtagh at the New Zealand Leather & Shoe Research Association (inc.) for assistance with the mechanical testing of the shoes used in this research.

Conflicts of Interest: The authors declare no conflicts of interest.

References

1. Lieberman, D.E.; Venkadesan, M.; Werbel, W.A.; Daoud, A.I.; D'Andrea, S.; Davis, I.S.; Mang'Eni, R.O.; Pitsiladis, Y. Foot strike patterns and collision forces in habitually barefoot versus shod runners. *Nature* **2010**, *463*, 531–535. [CrossRef]
2. Kasmer, M.E.; Liu, X.-C.; Roberts, K.G.; Valadao, J.M. Foot-Strike Pattern and Performance in a Marathon. *Int. J. Sports Physiol. Perform.* **2013**, *8*, 286–292. [CrossRef]
3. Damsted, C.; Larsen, L.H.; Nielsen, R.O. Reliability of video-based identification of footstrike pattern and video time frame at initial contact in recreational runners. *Gait Posture* **2015**, *42*, 32–35. [CrossRef]
4. Nishida, K.; Hagio, S.; Kibushi, B.; Moritani, T.; Kouzaki, M. Comparison of muscle synergies for running between different foot strike patterns. *PLoS ONE* **2017**, *12*, e0171535. [CrossRef]
5. Cavanagh, P.R.; Lafortune, M.A. Ground reaction forces in distance running. *J. Biomech.* **1980**, *13*, 397–406. [CrossRef] [PubMed]
6. Giandolini, M.; Poupard, T.; Gimenez, P.; Horvais, N.; Millet, G.Y.; Morin, J.-B.; Samozino, P. A simple field method to identify foot strike pattern during running. *J. Biomech.* **2014**, *47*, 1588–1593. [CrossRef] [PubMed]
7. Farley, C.T.; Gonzalez, O. Leg stiffness and stride frequency in human running. *J. Biomech.* **1996**, *29*, 181–186. [CrossRef] [PubMed]
8. Chan, Z.Y.S.; Au, I.P.H.; Lau, F.O.Y.; Ching, E.C.K.; Zhang, J.H.; Cheung, R.T.H. Does maximalist footwear lower impact loading during level ground and downhill running? *Eur. J. Sport Sci.* **2018**, *18*, 1083–1089. [CrossRef]
9. Nigg, B.M.; Liu, W. The effect of muscle stiffness and damping on simulated impact force peaks during running. *J. Biomech.* **1999**, *32*, 849–856. [CrossRef]
10. Nigg, B.M.; Bahlsen, H.A.; Luethi, S.M.; Stokes, S. The influence of running velocity and midsole hardness on external impact forces in heel-toe running. *J. Biomech.* **1987**, *20*, 951–959. [CrossRef]
11. Winter, D.A. Calculation and interpretation of mechanical energy of movement. *Exerc. Sport Sci. Rev.* **1978**, *6*, 183–256. [CrossRef] [PubMed]
12. Sinclair, J.; Richards, J.I.M.; Taylor, P.J.; Edmundson, C.J.; Brooks, D.; Hobbs, S.J. Three-dimensional kinematic comparison of treadmill and overground running. *Sports Biomech.* **2013**, *12*, 272–282. [CrossRef] [PubMed]
13. Kram, R.; Griffin, T.M.; Donelan, J.M.; Chang, Y.H. Force treadmill for measuring vertical and horizontal ground reaction forces. *J. Appl. Physiol.* **1998**, *85*, 764–769. [CrossRef] [PubMed]
14. Van Hooren, B.; Fuller, J.T.; Buckley, J.D.; Miller, J.R.; Sewell, K.; Rao, G.; Barton, C.; Bishop, C.; Willy, R.W. Is Motorized Treadmill Running Biomechanically Comparable to Overground Running? A Systematic Review and Meta-Analysis of Cross-Over Studies. *Sports Med.* **2020**, *50*, 785–813. [CrossRef]
15. Asmussen, M.J.; Kaltenbach, C.; Hashlamoun, K.; Shen, H.; Federico, S.; Nigg, B.M. Force measurements during running on different instrumented treadmills. *J. Biomech.* **2019**, *84*, 263–268. [CrossRef]
16. García-Pérez, J.A.; Pérez-Soriano, P.; Llana, S.; Martínez-Nova, A.; Sánchez-Zuriaga, D. Effect of overground vs treadmill running on plantar pressure: Influence of fatigue. *Gait Posture* **2013**, *38*, 929–933. [CrossRef]
17. Kluitenberg, B.; Bredeweg, S.W.; Zijlstra, S.; Zijlstra, W.; Buist, I. Comparison of vertical ground reaction forces during overground and treadmill running. A validation study. *BMC Musculoskelet. Disord.* **2012**, *13*, 235. [CrossRef]
18. Costa, M.E.F.; Fonseca, J.B.; Oliveira, A.I.S.D.; Cabral, K.D.D.A.; Araújo, M.D.G.R.D.; Ferreira, A.P.D.L. Prevalence and factors associated with injuries in recreational runners: A cross-sectional study. *Rev. Bras. Med. Esporte* **2020**, *26*, 215–219. [CrossRef]
19. Johnson, C.D.; Tenforde, A.S.; Outerleys, J.; Reilly, J.; Davis, I.S. Impact-Related Ground Reaction Forces Are More Strongly Associated with Some Running Injuries than Others. *Am. J. Sports Med.* **2020**, *48*, 3072–3080. [CrossRef]
20. Davis, S.I.; Bradley, J.B.; David, R.M. Greater vertical impact loading in female runners with medically diagnosed injuries: A prospective investigation. *Br. J. Sports Med.* **2016**, *50*, 887. [CrossRef]
21. Clarke, T.E.; Frederick, E.C.; Cooper, L.B. Effects of Shoe Cushioning upon Ground Reaction Forces in Running. *Int. J. Sports Med.* **1983**, *04*, 247–251. [CrossRef]
22. Bergstra, S.A.; Kluitenberg, B.; Dekker, R.; Bredeweg, S.W.; Postema, K.; Van den Heuvel, E.R.; Hijmans, J.M.; Sobhani, S. Running with a minimalist shoe increases plantar pressure in the forefoot region of healthy female runners. *J. Sci. Med. Sport* **2015**, *18*, 463–468. [CrossRef] [PubMed]

23. Kulmala, J.-P.; Kosonen, J.; Nurminen, J.; Avela, J. Running in highly cushioned shoes increases leg stiffness and amplifies impact loading. *Sci. Rep.* **2018**, *8*, 17496. [CrossRef] [PubMed]
24. Hannigan, J.J.; Pollard, C.D. Differences in running biomechanics between a maximal, traditional, and minimal running shoe. *J. Sci. Med. Sport* **2020**, *23*, 15–19. [CrossRef] [PubMed]
25. Almeida, M.O.; Davis, I.S.; Lopes, A.D. Biomechanical Differences of Foot-Strike Patterns During Running: A Systematic Review with Meta-Analysis. *J. Orthop. Sports Phys. Ther.* **2015**, *45*, 738–755. [CrossRef]
26. Shorten, M.; Mientjes, M.I.V. The 'heel impact' force peak during running is neither 'heel' nor 'impact' and does not quantify shoe cushioning effects. *Footwear Sci.* **2011**, *3*, 41–58. [CrossRef]
27. Gruber, A.H.; Boyer, K.A.; Derrick, T.R.; Hamill, J. Impact shock frequency components and attenuation in rearfoot and forefoot running. *J. Sport Health Sci.* **2014**, *3*, 113–121. [CrossRef]
28. Gruber, A.H.; Edwards, W.B.; Hamill, J.; Derrick, T.R.; Boyer, K.A. A comparison of the ground reaction force frequency content during rearfoot and non-rearfoot running patterns. *Gait Posture* **2017**, *56*, 54–59. [CrossRef]
29. Williams, D.S.; McClay, I.S.; Manal, K.T. Lower Extremity Mechanics in Runners with a Converted Forefoot Strike Pattern. *J. Appl. Biomech.* **2000**, *16*, 210–218. [CrossRef]
30. Shih, Y.; Lin, K.-L.; Shiang, T.-Y. Is the foot striking pattern more important than barefoot or shod conditions in running? *Gait Posture* **2013**, *38*, 490–494. [CrossRef]
31. Macdermid, P.W.; Walker, S.J.; Cochrane, D. The Effects of Cushioning Properties on Parameters of Gait in Habituated Females While Walking and Running. *Appl. Sci.* **2025**, *15*, 1120. [CrossRef]
32. Renner, K.E.; Peebles, A.T.; Socha, J.J.; Queen, R.M. The impact of sampling frequency on ground reaction force variables. *J. Biomech.* **2022**, *135*, 111034. [CrossRef] [PubMed]
33. Welch, P. The use of fast Fourier transform for the estimation of power spectra: A method based on time averaging over short, modified periodograms. *IEEE Trans. Audio Electroacoust.* **1967**, *15*, 70–73. [CrossRef]
34. Zhuang, Y.; Zhou, W.; Zeng, Z.; Mo, S.; Wang, L. Influences of footstrike patterns and overground conditions on lower extremity kinematics and kinetics during running: Statistical parametric mapping analysis. *PLoS ONE* **2025**, *20*, e0317853. [CrossRef] [PubMed]
35. Kulmala, J.-P.; Avela, J.; Pasanen, K.; Parkkari, J. Forefoot strikers exhibit lower running-induced knee loading than rearfoot strikers. *Med. Sci. Sports Exerc.* **2013**, *45*, 2306–2313. [CrossRef] [PubMed]
36. Nigg, B.M.; Vienneau, J.; Smith, A.C.; Trudeau, M.B.; Mohr, M.; Nigg, S.R. The Preferred Movement Path Paradigm: Influence of Running Shoes on Joint Movement. *Med. Sci. Sports Exerc.* **2017**, *49*, 1641–1648. [CrossRef]
37. Di Michele, R.; Merni, F. The concurrent effects of strike pattern and ground-contact time on running economy. *J. Sci. Med. Sport* **2014**, *17*, 414–418. [CrossRef]
38. Sobhani, S.; van den Heuvel, E.R.; Dekker, R.; Postema, K.; Kluitenberg, B.; Bredeweg, S.W.; Hijmans, J.M. Biomechanics of running with rocker shoes. *J. Sci. Med. Sport* **2017**, *20*, 38–44. [CrossRef]
39. Milner, C.E.; Ferber, R.; Pollard, C.D.; Hamill, J.; Davis, I.S. Biomechanical factors associated with tibial stress fracture in female runners. *Med. Sci. Sports Exerc.* **2006**, *38*, 323–328. [CrossRef]
40. Rodrigo-Carranza, V.; Hoogkamer, W.; González-Ravé, J.M.; Horta-Muñoz, S.; Serna-Moreno, M.d.C.; Romero-Gutierrez, A.; González-Mohíno, F. Influence of different midsole foam in advanced footwear technology use on running economy and biomechanics in trained runners. *Scand. J. Med. Sci. Sports* **2024**, *34*, e14526. [CrossRef]
41. Mann, R.; Malisoux, L.; Urhausen, A.; Statham, A.; Meijer, K.; Theisen, D. The effect of shoe type and fatigue on strike index and spatiotemporal parameters of running. *Gait Posture* **2015**, *42*, 91–95. [CrossRef]
42. Sun, X.; Yang, Y.; Wang, L.; Zhang, X.; Fu, W. Do Strike Patterns or Shoe Conditions have a Predominant Influence on Foot Loading? *J. Hum. Kinet.* **2018**, *64*, 13–23. [CrossRef] [PubMed]
43. Mercer, J.A.; Horsch, S. Heel–toe running: A new look at the influence of foot strike pattern on impact force. *J. Exerc. Sci. Fit.* **2015**, *13*, 29–34. [CrossRef] [PubMed]
44. Napier, C.; Fridman, L.; Blazey, P.; Tran, N.; Michie, T.V.; Schneeberg, A. Differences in Peak Impact Accelerations Among Foot Strike Patterns in Recreational Runners. *Front. Sports Act. Living* **2022**, *4*, 802019. [CrossRef] [PubMed]